Available online www.jsaer.com

***Journal of Scientific and Engineering Research*, 2020, 7(5):332-343**

Research Article

ISSN: 2394-2630
CODEN(USA): JSERBR

Mapping the hydrodynamic characteristics of the North Shore aquifer system using the theory of regionalized variables: special case of transmissivity

Ahmeth L. Diakhate[1], Ababacar Fall[1*], Saïdou Ndao[1,2], Papa B. D. Thioune[1,3], El hadji B. Diaw[1], Mamadou Wade[1]

[1]Laboratory of Science and Technology of Water and Environment (LaSTEE), Polytechnic School of Thiès BP A 10 Thiès, Senegal
[2]University of Thiès, UFR Sciences and Technologies, Cité Malick Sy, PB 967, Thiès, Senegal
[3]University of Thiès, Higher Institute of Agricultural and Rural Training (ISFAR) PO Box 54, Bambey, Senegal

Abstract In this work, we present a geostatistical modelling methodology that allows the analysis of spatial variability and the estimation of transmissivity values of the aquifer system of the northern coast of Senegal. This study is carried out with the GIS tool, on the basis of the values observed in 83 boreholes located in the study area, including 40 at the Maestrichtian level, 26 at the terminal continental level and 17 at the Quaternary level. Experimental variogram types have been produced that take into account the isotropic aspect and make it possible to infer spatial correlations between the values. These variograms were modelled using two types of analytical functions: Gaussian and spherical. The performance of this modeling was evaluated through the analysis of estimation errors calculated by the cross-validation method. The results obtained correspond to thematic maps that are used for decision making and for the realization of a hydrogeological model for the slick of the northern coast of Senegal.

Keywords Geostatistical modeling, GIS, variograms, transmissivity, northern coastal aquifer system

1. Introduction

In the Sahel, water is the major limiting factor for both human food and agricultural production. In Senegal, despite a semi-arid climate, the problem of water is a development issue. The scarcity of surface water and the unsustainability of this resource due to the unfavourable climatic conditions of recent decades have favoured the use of groundwater to satisfy the water needs of the population. These aquifers are in great demand for the water supply of populations. However, the constant increase in the number of boreholes tapping the aquifer inevitably leads to a problem of water management and therefore a rational and intelligent exploitation of this aquifer is essential. This requires, first of all, knowledge of the geometry of the aquifer, but also of its hydrodynamic characteristics, including transmissivity, which is essential [1].

Thus, the values of this type of parameters are only known in some sites where a network of pump test measurements is available. The latter is necessarily of limited density, given the constraint linked to the significant costs generated by their implementation, which does not always make it possible to multiply the tests satisfactorily in space and time.

The aim of this work is to map the transmissivity of the aquifer system of the north coast of Senegal, the deep aquifers of the Maestrichtian, the terminal continental and the Quaternary sands between Kayar and Saint-Louis, using geostatistical methods with Kriging as an estimator [2]. Indeed, kriging provides a quantitative mapping of optimal point or zonal estimates [3]. It is a weighting method on available data, where the weighting mode is

strictly related to the field characteristics recognized in a geostatistical description ([4];[5];[6]). Geostatistical methods are widely used in the field of hydrogeology and water sciences in general ([7] [8] [9] [10] [11]) and will enable us to better identify the potential of this water table and provide a valuable management tool for decision-makers [12].

2. Materials and Method

2.1. Presentation of the study area

The northern coastline extends over the northwestern part of Senegal and partially covers the administrative regions of Dakar, Thiès, Louga and Saint-Louis (Figure 1). Bordering the maritime fringe of the north of the country, it is bounded in its inland part by the Dakar-Saint-Louis national road (N2), to the west by the Atlantic Ocean, to the east by the 16°10' meridian which passes through Diourbel, to the north and south respectively by the 16°00' and 14°30' parallels. It extends over a length of 180 km, and its width varies from 5 to 30 km inland [12]. This narrow strip of the Atlantic coast has an area of about 2300 km² [13] and is called the Niayes region. It is an area characterized by dunes and depressions often flooded by the outcrop of the groundwater table.

2.2. Description of the aquifer

Hydrogeological studies [14] [15] carried out on the northern coast have revealed the presence of the following formations respectively from bottom to top: Maestrichtian, Paleocene, Eocene, Continental Terminal and Quaternary (Figure 2).

We can group these aquifers into 3 large systems corresponding to the main geological formations.

- - The shallow aquifer system which includes the predominantly sandy-clayey formations of the Quaternary and Continental Terminal.
- - The intermediate aquifer system made up of two predominantly calcareous formations: the Eocene present throughout the basin and the Paleocene located only in the Horst of Ndiass and in the Mbour region.
- - The Deep Aquifer system which concerns the only formation of the Maestrichtian sands.

In this study, we focus only on shallow and deep aquifer systems because of their importance in the groundwater resources of the north coast [16].

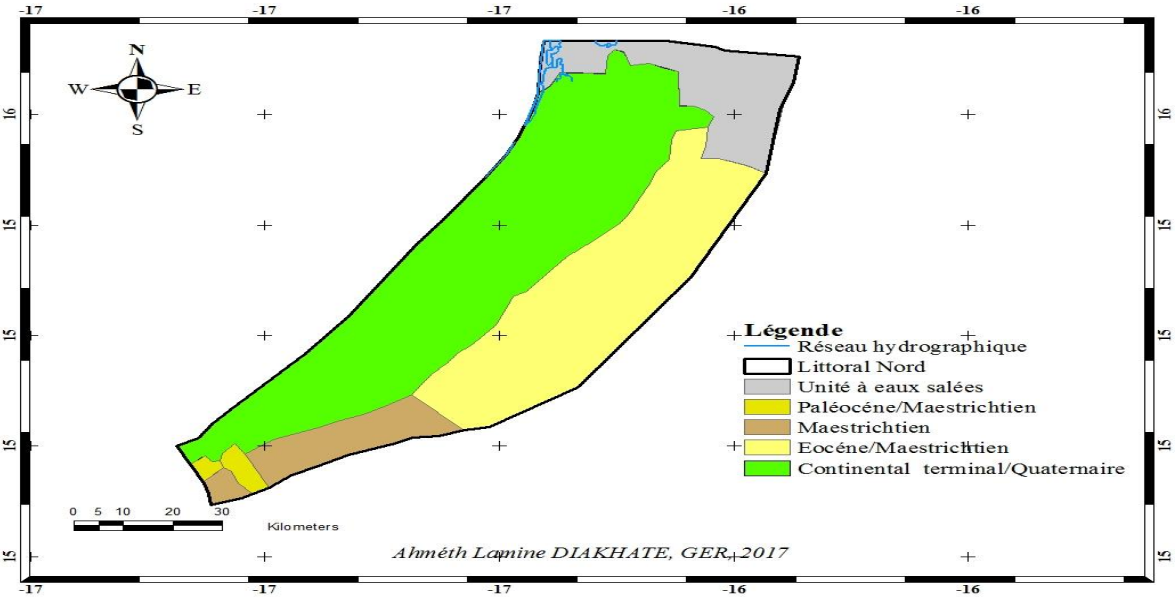

Figure 2: Map of North Shore Aquifer Units

2.3. Geostatistical Approach: Krigging Interpolation

Kriging is a spatial interpolation method that takes into account the geometric configuration of the observed points and the spatial structure of the estimated variable. In addition to the estimation itself, kriging allows the uncertainty to be evaluated. Unlike all other methods, Kriging also allows us to calculate the estimation error.

Thus, to be able to apply the results of the theory of random functions, it is necessary to go through statistical inference. This is only possible if there are a sufficient number of achievements. Statistical inference then requires the introduction of additional hypotheses on the random function to remove the impossibility.
Two assumptions are often made in order to make statistical inference:

- the hypothesis of ergodicity or stationarity of order 2 where we can then assume that each particular realization is sufficient to account for all the possible realizations;
- and the intrinsic hypothesis where we will thus be satisfied to make the hypothesis that, for any vector h, the increase Z(x+h) - Z(x) has a mathematical expectation of zero and a variance independent of the point with the random variable.

$$\begin{cases} E[Z(x+h)-Z(x)]=0 \\ Var[Z(x+h)-Z(x)]=2\gamma(h) \end{cases} \quad (1)$$

The function is called "semi-variogram", often referred to as a variogram. Thus the random function describing the transmissivity of our aquifer will be considered as an intrinsic random function.
Geostatistics mainly uses as descriptors the variogram and the covariance function, which are also called structure functions. The variogram of an intrinsic random function is thus by definition:

$$\gamma(h)=\frac{1}{2}Var[Z(x+h)-Z(x)] \quad (2)$$

Assuming that the intrinsic hypothesis is satisfied, the variogram is estimated by the experimental variogram from the pairs of experimental points available on the only accessible realization:

$$\gamma^*(h)=\frac{1}{2n(h)}\sum_{i=1}^{n(h)}[z(x_i+h)-z(x_i)]^2 \quad (3)$$

With $\gamma^*(h)$: the variogram estimator;

h : the average separation distance between the pairs of the class ;

$z(x_i)$ and $z(x_i+h)$: the values of z in x_i et x_{i+1} ;

$n(h)$: the number of couples in the class.

The methodology adopted in this work has been endorsed by many authors: [17] [18] [19] [20]. The mapping methods used are those proposed by the Geostatistical Analyst extension of ArcGIS 10.2. The information on different boreholes were entered into a spatial database containing all the hydrogeological parameters that characterize the studied aquifer of the northern littoral [21]; then we established a geostatistical model for the fields of the studied parameter by going through the following steps:

- Data Mining ;
- Construction of an experimental variogram;
- Development of a synthetic structural model;
- Cross-validation of the model;
- Ordinary kriging mapping.

3. Results and Discussions

3.1. Maestrichtian Deep Aquifer System

3.1.1. Exploratory analysis of transmissivity data

The input data is a 40-point sample. They are collected from the Senegalese Direction of Water Resources Management and Planning (DGPRE). The distribution of these samples across the northern coast is illustrated in Figure 2. The transmissivity values of the sample were obtained by pumping test.
The map of the location of these data, drawn with symbols proportional to the value of the transmissivities, shows that the latter have a certain spatial continuity (spatial autocorrelation). Moreover, the low values are located rather close to the coast and in the south-east and the high values in the north of the area (Figure 3).

The analysis of Figure 3 shows that in the Niayes region, the values of transmissivity at the level of the Maestrichtian are in the range [0.48.10^{-4} m^2/s; 2.7. 10^{-2} m^2/s] for a mean of 6.52.$10^{-3}m^2$/s with a standard deviation of 0.674.10^{-2}.

The distribution of the data, illustrated by the histogram in Figure 4, shows that the kurtosis coefficient (k=6.126) is well above 0, implying that the distribution reaches a maximum level. The skewness coefficient with a value of 1.8013 indicates that this distribution is not symmetrical, it is shifted to the left.

The histogram of the transmissivity data shows a tail towards the high values and an asymmetrical shape.

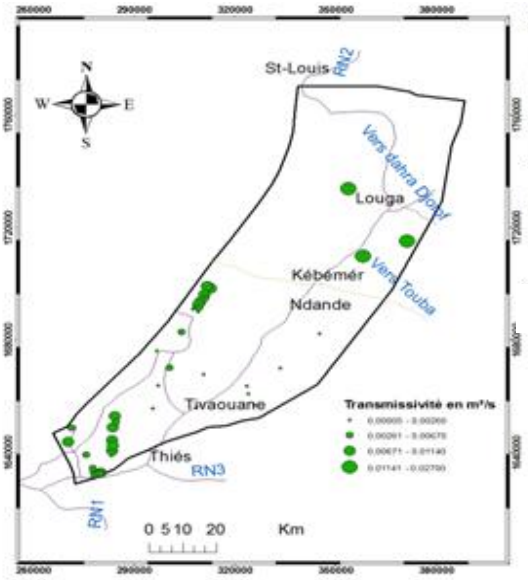

Figure 3: Data Location Map

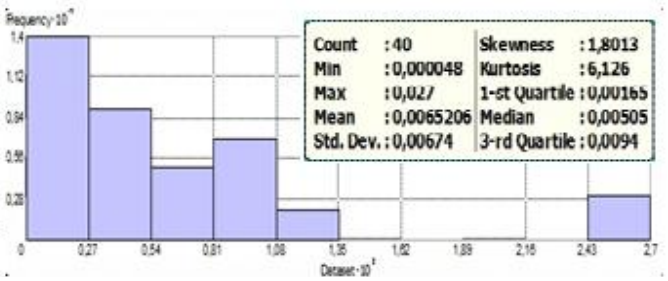

Figure 4: Statistical characteristics of the sample

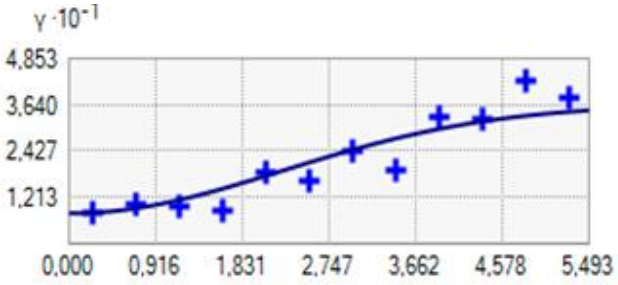

Figure 5: Experimental variogram plot

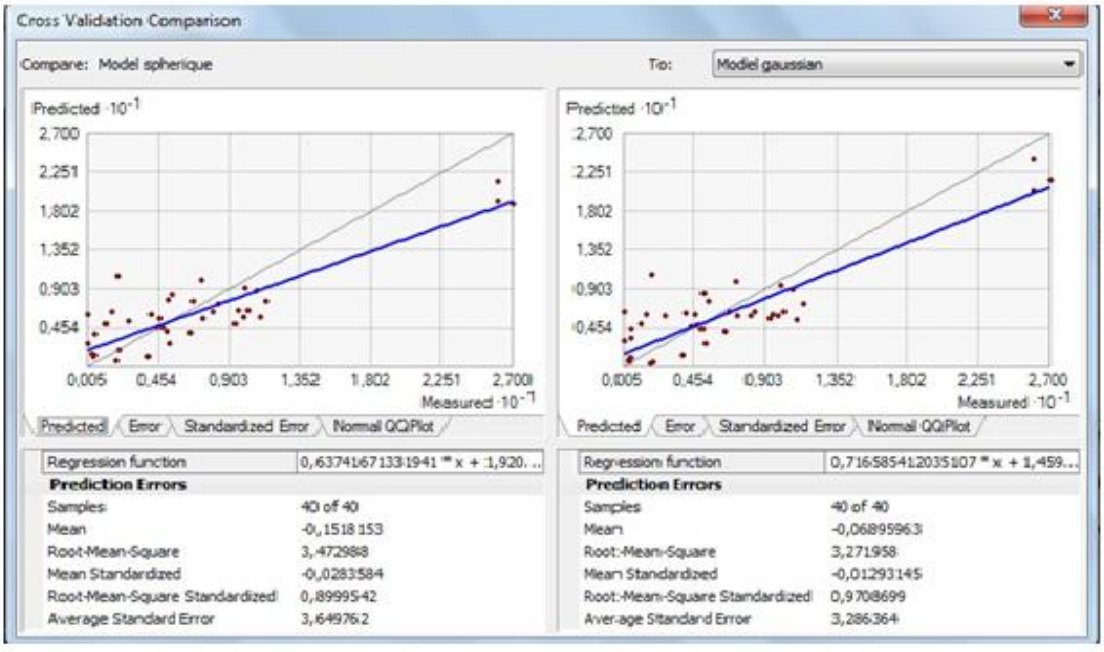

Figure 6: Cross-validation results

3.1.2. Construction of the experimental variogram

In order to construct the experimental variogram, a constant step h equal to 45.7 m was selected. This step is the difference between two distances for which a value is calculated in the variogram. With this step size, 12

distance classes are obtained, represented on the variogram by their mean values. Each point is obtained from a number of pairs of points in the sample (Figure 5).

3.1.3. Variogram modelling

The adjustment of the points of the experimental variogram is obtained using the weighted least squares method. Thus, concerning the study of transmissivity, the theoretical variogram (in [m²/s]²) obtained is Gaussian combined with a nugget effect of the order of 7.976; an a priori variance of 28.45 and has a plateau at 552 m (Figure 4). Since the deep Maestrichtian aquifer consists almost everywhere of sand, an isotropic model is chosen.

3.1.4. Validation of the adopted structural model

Frequently used in geostatistics [22], it allows to compare the impact of different models and to choose one for the estimation. Its principle consists in re-estimating the values of transmissivity for the sampled points by means of the adjusted models. The operation is carried out for all points, and the quality of the estimate is calculated on the basis of five statistical criteria used by the ArcGis software [23].

- average error : $\frac{1}{n}\sum_{i=1}^{n}[Z^*(x_i) - Z(x_i)]$ (4)

- standard deviation of errors : $\sqrt{\frac{1}{n}\sum_{i=1}^{n}[Z^*(x_i) - Z(x_i)]^2}$ (5)

- mean standard deviation : $\sqrt{\frac{1}{n}\sum_{i=1}^{n}\hat{\sigma}(x_i)}$ (6)

- mean reduced error : $\frac{1}{n}\sum_{i=1}^{n}[Z^*(x_i) - Z(x_i)]/\hat{\sigma}(x_i)$ (7)

- standard deviation of the reduced error : $\sqrt{\frac{1}{n}\sum_{i=1}^{n}\left[[Z^*(x_i) - Z(x_i)]/\hat{\sigma}(x_i)\right]^2}$ (8)

$Z^*(x_i)$: value we are trying to predict for a place;
$Z(x_i)$: estimation of the measured value;
$\hat{\sigma}(x_i)$: standard error of prediction;
n : number of points used for cross-validation, $n = 40$;
This technique considers the model to be efficient when:

- the mean of the estimation errors and the reduced (standardized) errors are close to zero, which verifies that the kriging is unbiased and reflects the good precision of the estimator;
- the standard deviation of the reduced error is close to 1 and the standard deviation of the errors is close to the mean of the kriging standard deviation [24].

Table 1: Summary table of cross-validation results

Statistical parameters	Spherical model	Gaussian model
Average estimation errors	-0.1518	-0.0689
Standard deviation of estimation errors	3.4729	3.2719
Reduced Mean Error	-0.0283	-0.0129
Standard deviation of reduced errors	0.899	0.97
Mean standard deviation	3.649	3.286

This table shows the values obtained from the errors of the two models. The results vary considerably from one model to the other. The Gaussian model of the isotropic variogram makes the estimate globally unbiased, as its mean of the estimation errors and reduced (standardized) errors are closer to zero (-0.069) and (-0.0129). However, for the Spherical model, the mean error of the estimate is large. The standard deviation of the error of the Gaussian model is closer to 1 than the Spherical model (0.97) and (0.89). The standard deviation of Gaussian model errors is closer to the mean of the kriging standard deviation (3.27 and 3.28). The latter model is the winner of this comparison and its parameters will be used for the interpolation, by ordinary kriging, of the transmissivity values of the Maestrichtian slick of the north shore.

3.1.5. Kriging interpolation

After validating the Gaussian model of the isotropic variogram with a range equal to 552 m and a bearing equal to 36.4, the interpolation was performed using ordinary kriging. This type of Kriging, which does not require knowledge of the expectation of the regionalized variable, is an exact interpolation method [19] which preserves the regionalized values measured at the level of the boreholes. Figure 6 shows the spatial distribution of the values of the transmissivity of the deep aquifer system obtained by this geostatistical modelling. The values are between 0.00021 and 0.02693 m²/s. They are high in most of the deep aquifer system in the north and are very low towards the centre and south of the area with values below 0.02 m²/s.

The estimation errors calculated by ordinary kriging are shown in Figure 7. Examination of the latter shows that the low values of the estimation error are located in the centre and south of the Study Area. This is related to the high number of observed values existing in these locations of the aquifer. On the other hand, the error becomes more and more important on the rest of the slick, especially towards the North where the transmissivity values remain unknown due to the low number of structures tested in these places.

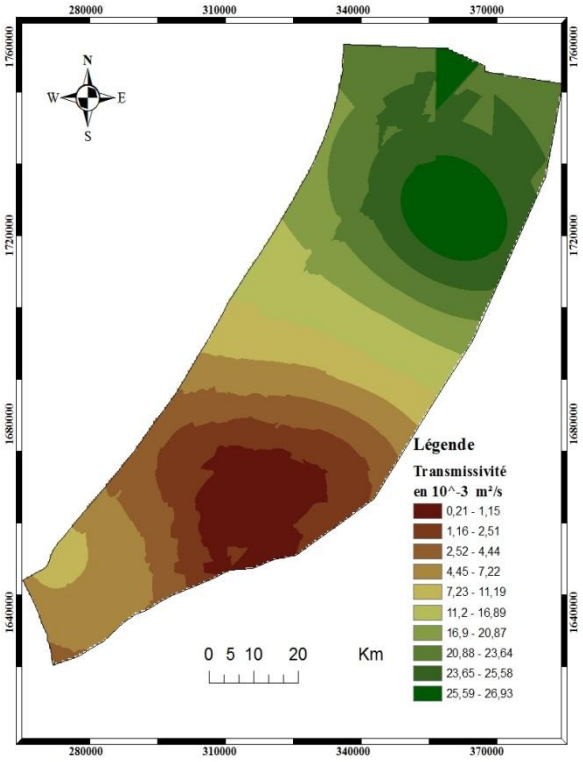

Figure 7 : Map of estimated transmissivity values

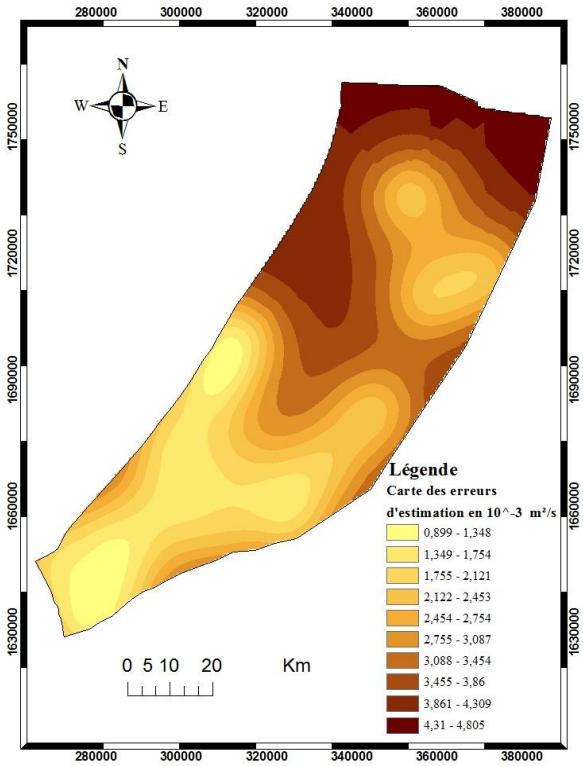

Figure 8: Map of errors in estimating transmissivity values

3.2. Superficial Aquifer System: Terminal Continental

3.2.1. Exploratory analysis of transmissivity data

Exploration of the input data from 26 observation points is illustrated in Figures 8, 9 and 10. Their analyses show that in the Niayes region, the values of transmissivity at the terminal continental level are in the range [$3.8.10^{-4}$ m^2/s; $5.7.\ 10^{-2}$ m^2/s] for a mean of $1.92.10^{-2}$ m^2/s with a standard deviation of $1.65.10^{-2}$. The histogram (Figure 10) of transmissivity shows the presence of some very high values and gives an asymmetry coefficient (skewness = 0.47) which is positive. The kurtosis coefficient (k = 2.376) is greater than 0, the distribution reaches a maximum level.

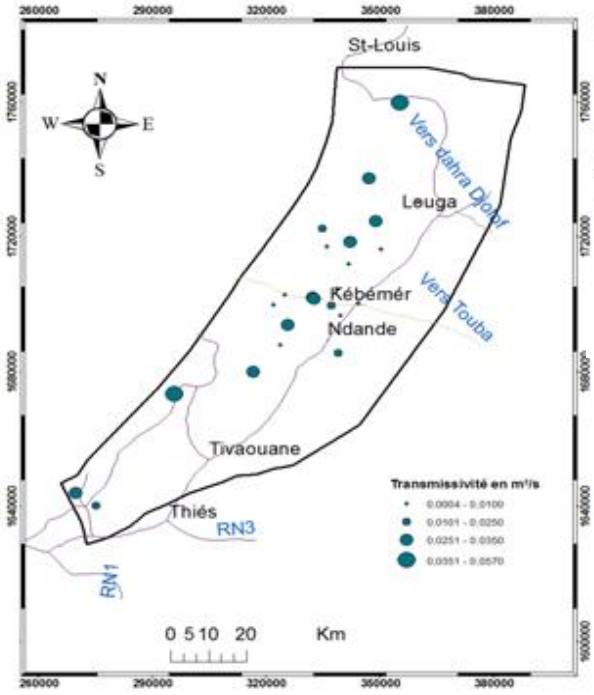

Figure 9: Map of data location

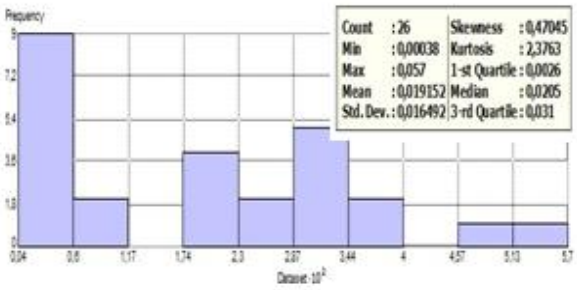

Figure 10: Some characteristics of the sample

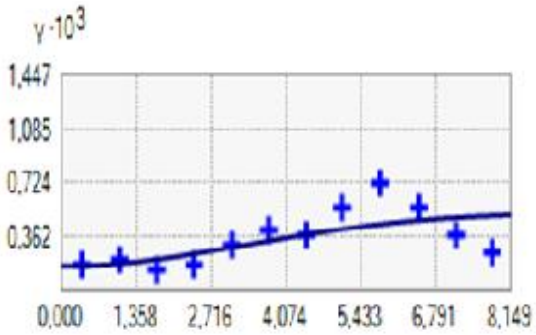

Figure 11: Plot of the variogram

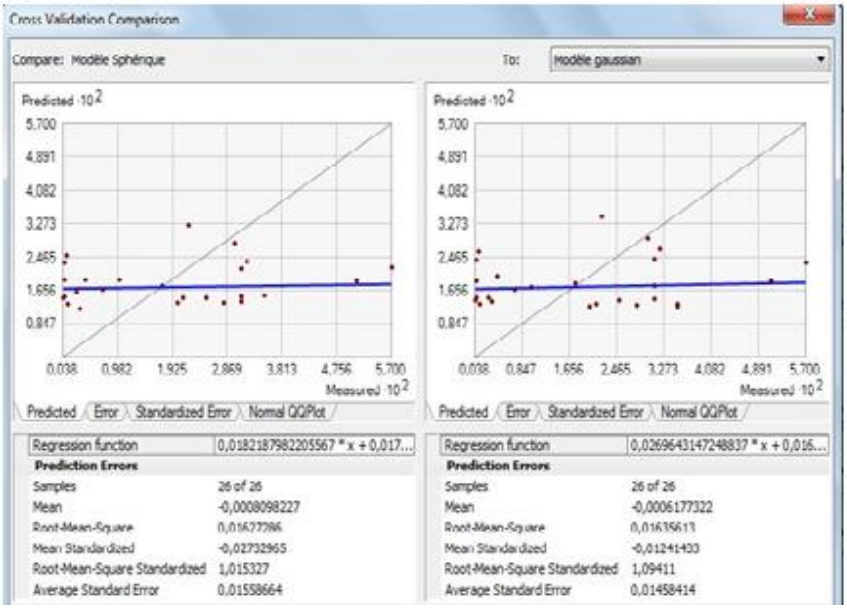

Figure 12: Result of the cross-validation

3.2.3. Construction of the experimental variogram

The variogram characterizes the spatial continuity of the regionalized variable. Figure 11 shows the omnidirectional experimental variogram, calculated for multiple distances at 68-metre intervals. With this step size, we obtain 12 distance classes represented on the variogram by their mean values.

3.2.4. Variogram modelling

The omnidirectional variogram reaches a plateau at a distance of 815 meters as a range for the spherical method. It can be deduced that the regionalized variable (transmissivity) is a realization of a stationary random function of order 2 [25].

In the analysis, the variogram of the transmissivity values shows a discontinuity at the origin showing the local irregularity of the transmissivity with a nugget effect of the order of 0.000166 and has an a priori variance of 0.000248 (Figure 11).

3.2.5. Validation of the adopted structural model

As in the Maastrichtian, the spherical model of the variogram has a mean of the estimation errors and reduced (standardized) errors (-0.00809) and (-0.0273) which are close to zero. Its standard deviation of the reduced error is closer to 1 and its standard deviation of the errors is closer to the mean of the kriging standard deviation (0.0163) ≈ (0.0155), compared to the Gaussian model. The spherical model wins in this comparison (Table 2).

Table 2: Summary table of cross-validation results

Statistical parameters	Spherical model	Gaussian model
Average estimation errors	-0.000809	-0.000617
Standard deviation of estimation errors	0.01627	0.1635
Reduced Mean Error	-0.0273	-0.0124
Standard deviation of reduced errors	1.0153	1.0941
Mean standard deviation	0.01558	0.0145

This approach allowed us to validate our variogram model against the experimental variogram and to incorporate them into the kriging interpolation for the estimation of transmissivity values.

3.2.6. Kriging interpolation

After validating the spherical model of the isotropic variogram with a range equal to 815 m and a bearing equal to 41.10^{-5}, the interpolation was performed with ordinary kriging.

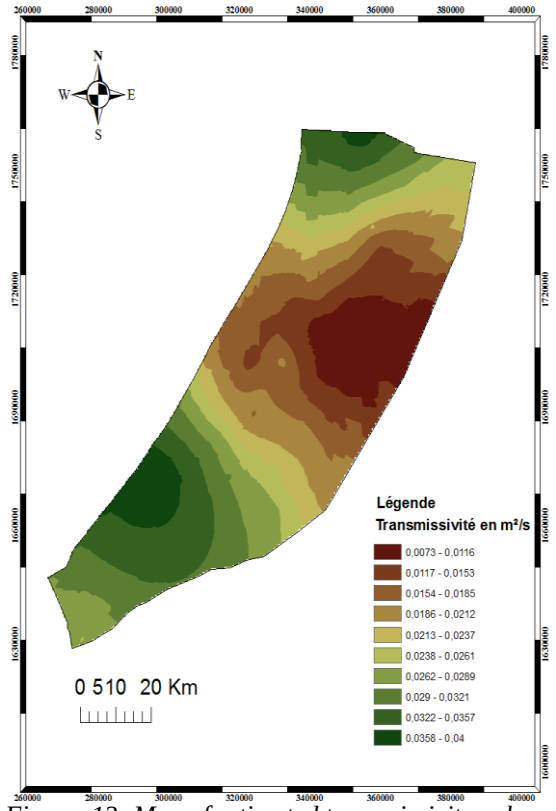

Figure 13: Map of estimated transmissivity values

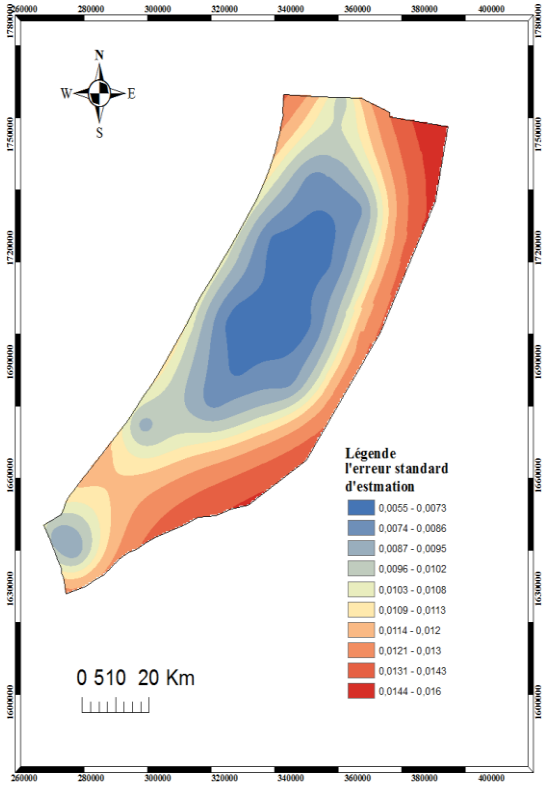

Figure 14: Map of errors in estimating transmissivity values

Figure 12 shows the spatial distribution of the transmissivities (in m²/s) of the terminal continental aquifer deduced from the estimated values by kriging. This map shows that the most transmissive sectors are located entirely to the south and an extreme part of the northwest of the Study Area. The lowest transmissivity values are located in the centre of the slick, more particularly in the east. The map of the error estimate (Figure 14)

shows that the error of the estimate is fairly small in the centre of the slick. In contrast, the error becomes smaller near the slick boundaries, due to the low number of structures tested at these locations.

3.3. Superficial Aquifer System: The Quaternary

3.3.1. Exploratory analysis of transmissivity data

The input data is a 17-point sample. The histogram (Figure 16) of transmissivity gives an asymmetry coefficient (skewness=0.816) to indicate that this distribution is not symmetrical. The kurtosis coefficient (k=2 .8175). The histogram of the transmissivity data shows a tail towards the high values and an asymmetric shape. The set of values constitutes, in the statistical sense, a single population with a normal distribution, and centred on the value $2.69.10^{-2}$ m^2/s.

3.3.2. Construction of the experimental variogram

Figure 17 shows the omnidirectional experimental variogram, calculated for multiple distances of a 35-metre pitch. With this step size, we obtain 12 distance classes represented on the variogram by their mean values.

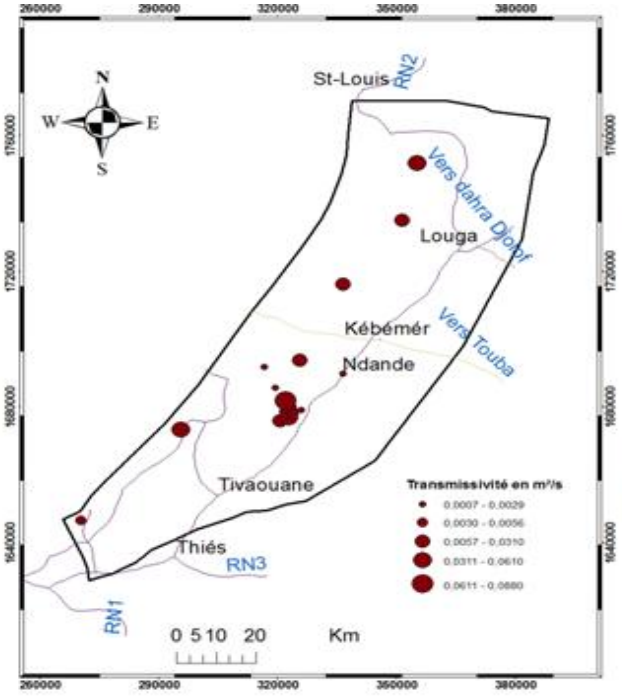

Figure 15: Data Location Map

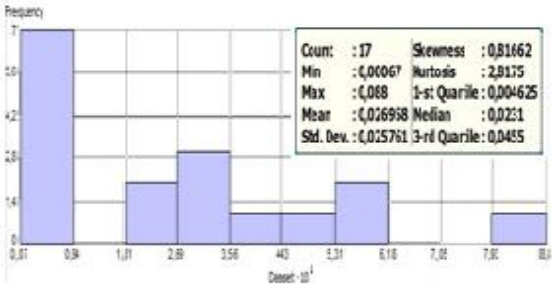

Figure 16: Some characteristics of the sample

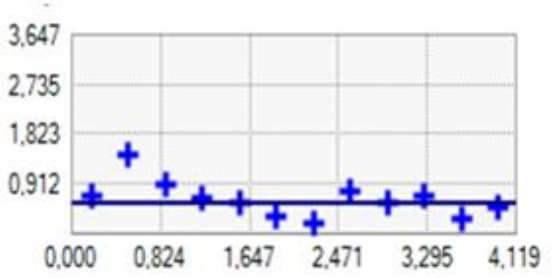

Figure 17: Plot of the variogram

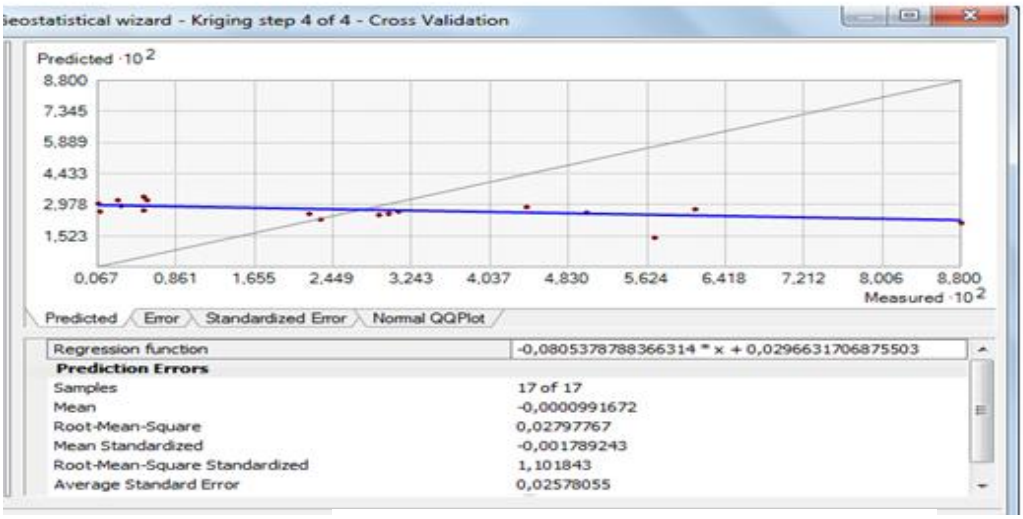

Figure 18: Result of the cross-validation

3.3.3. Variogram m

On analysis, the variogram of transmissivity values shows a discontinuity at the origin showing local irregularity of transmissivity with a pure nugget effect of the order of 0.0005678. However, for our study, we will use the linear model, which has a better calibration.

3.3.4. Validation of the adopted structural model

In order to obtain an efficient model, we modified the model parameters until the optimal values for the linear model were obtained. The new cross-validation shows us that:

The mean of the estimation errors and the reduced (standardized) errors are close to zero (-0.000099) and (-0.001790) respectively; the standard deviation of the reduced error is close to 1 (1.1018) and the standard deviation of the errors is close to the mean of the kriging standard deviation (0.0279≈0.0257) (Table 3).

Table 3: Summary table of cross-validation results

Statistical parameters	Linear Model
Average estimation errors	-0.000099
Standard deviation of estimation errors	0.027977
Reduced Mean Error	-0.001789
Standard deviation of reduced errors	1.101843
Mean standard deviation	0.02578

3.3.5. Kriging interpolation

Figure 19 shows the spatial distribution of transmissivities (in m²/s) of the Quaternary aquifer inferred from kriging estimates. The high transmissivity values (T≥0,025 m²/s) are practically distributed in the north, south and centre of the area. The lowest transmissivity values (T≤0,025 m²/s) are also distributed close to the coastal limit and slightly towards the centre of the aquifer. The error estimation map (Figure 20) shows that the error of the estimation is rather small in the centre of the slick. On the contrary, the error becomes less small near the limits, the whole southern and northern part of the slick.

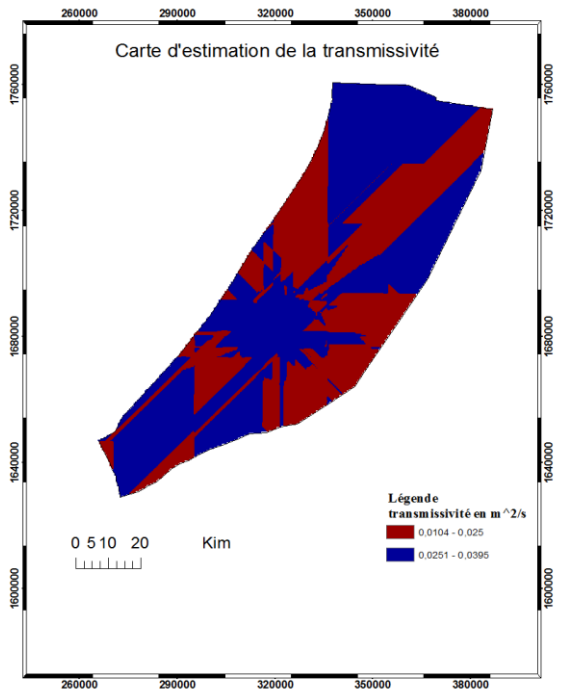

Figure 19: Map of estimated transmissivity values

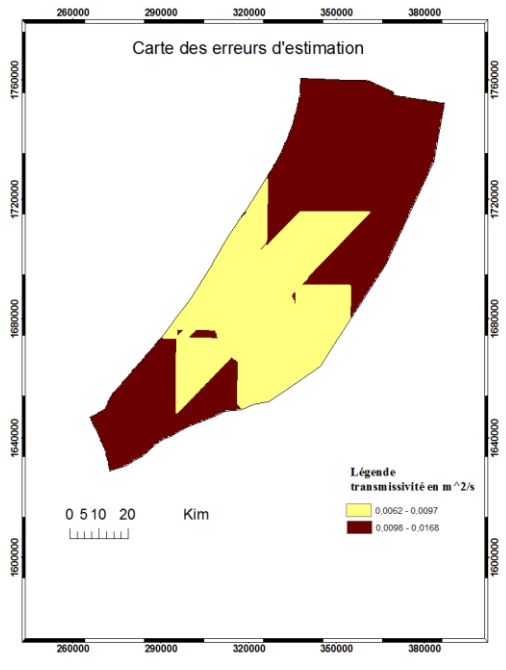

Figure 20 : Map of errors in estimating transmissivity values

4. Conclusion

In this study, geostatistical modeling was applied to the transmissivity values collected from a set of boreholes that capture the slicks of the northern shoreline more particularly at the level of the Maestrichtian, the terminal continental and the Quaternary. This probabilistic methodology made it possible to produce more reliable maps for estimating transmissivity. This estimate was made using the optimal method of ordinary kriging, which provided an indication of the error in each estimated value. This tool also made it possible to quantify the uncertainty due to interpolation. Interpolation by ordinary kriging with the Gaussian model at the Maestrichtian level, spherical for the terminal continental and linear at the Quaternary level gave a good prediction of a mean error close to zero. Indeed, the estimation error map obtained from this study can provide guidance for the selection of new observation sites to improve the quality of the forecast. The aquifer transmissivity maps thus obtained are certainly an important and necessary decision-making tool, particularly for the development and management of water resources, in this case the choice of the most favourable locations for future exploitation works (wells, boreholes, etc.), in order to meet the region's ever-increasing needs for drinking and agricultural water.

References

[1]. G. De Marsily. Hydrologie quantitative, Collection Sciences de la terre, Masson, Paris, 215p, 1981

[2]. Krige. (1951): A statistical approach to some basic mine valuation problem son the Witwatersr and. Journal of the Chemical, Met allurgical and Mining Society.

[3]. J.P. DELHOMME. Application de la théorie des variables régionalisées dans les sciences de l'eau. Bull. BRGM, 2 (III), 4, pp. 341-375, 1978.

[4]. Ch. Gascuel-Odoux. Application de géostatistique à l'étude de la variabilité spatiale des propriétés hydriques du sol. Thèse de doctorat ingénieur, ENSM de Paris, 235p, 1984.

[5]. M. Voltz. Variabilité spatiale des propriétés physiques du sol en milieu alluvial. Essai de cartographie quantitative des paramètres hydrodynamiques. Thèse de doctorat ingénieur, ENSA de Montpellier, Décembre 1986.

[6]. A. Martela. Estimation des flux hydriques et nitriques dans les sols agricoles. Approche spatiale à plusieurs échelles dans la plaine du Rhin supérieur; Thèse de Doctorat, Université Louis Pasteur, Strasbourg, 1993.

[7]. ASCE. Review of geostatistics in geohydrology 1: basic concepts, 2: applications. American society of Civil Enginers Task committee on Geostatistical Techniques in Geohydrology. ASCE J Hydraul Eng 116 (5): 612-658, 1990.

[8]. Ch. Gascuel-Odoux. Application de géostatistique à l'étude de la variabilité spatiale des propriétés hydriques du sol. Thèse de doctorat ingénieur, ENSM de Paris, 235p, 1984.

[9]. Asce 1990. Review of geostatistics in geohydrology1: basic concepts, 2: applications. American society of Civil Engineers Task committee on Geostatistical.

[10]. Munoz Pardo J. F. 1987. Approche géostatistique de la variabilité spatiale des milieux géophysiques : Application à l'échantillonnage des phénomènes bidimensionnels par simulation d'une fonction aléatoire. Thèse de doctorat ingénieur, Université Joseph Fourier, Grenoble. p. 229.

[11]. Russo D. 1984. Design if optimal sampling networks for estiming the variogram; Soil Sci. Soc. Am. J. 48, pp. 708-716, 1984.

[12]. E.B. Diaw et al. 2016. Geostatistical approach for mapping the transmissivity of the senegalese deep aquifer system.Vol. 5, no. 2, december 2016 issn 2305-493x ARPN Journal of Earth Sciences ©2006-2016 Asian Research Publishing Network (ARPN). All rights reserved.

[13]. Kane, C. H. (1995) : Contribution à l'étude hydrochimique de la nappe des sables Quaternaires du littoral nord du Sénégal entre Kayar et Saint-Louis. Thèse de Doctorat, Université cheikh Anta diop de Dakar, 131p.

[14]. Diouf, S. (1995) : Application de la géophysique (électrique et sismique) à l'étude de la géométrie du réservoir de l'aquifère du littoral nord Sénégal (de Taïba à Rao). Mémoire de DEA. Université de Dakar (Facultés des Sciences, Département de géologie): 154p.

[15]. Noël, Y. (1975) : Etude hydrogéologique des calcaires lutétiens de la région de Bambey (1ère phase). Dak 01: 47.
[16]. Ministère de l'Hydraulique et de l'assainissent, DGPRE, Étude du Plan de Gestion des Ressources en Eau de la Sous UGP Niayes RAPPORT DE SYNTHESE, IDEV - ic & EDE International, Novembre 2014.
[17]. Rentier. (2002): Méthode Stochastique de délimitation des zones de protection au tour des captages d'eau, Thèse de doctorat, Université de Liège
[18]. El morjani Z. (2003): Conception d'un système d'information à référence spatiale pour la gestion environnementale ; application à la sélection de sites potentiels de stockage de déchets ménagers et industriels en région semi-aride (Souss, maroc). Thèse de la faculté des sciences de l'université de Genève n° 3370, 283 p.
[19]. Bailladgeon, S. (2005) : Le krigeage : revue de la théorie et application à l'interpolation spatiale de données de précipitations. Mémoire pour l'obtention du grade (M.Sc.). Université Laval Québec.106 p.
[20]. Jarar, O. H., Hydris. (2009) : Un système d'information géospatiale pour une gestion durable des ressources en eaux souterraines. Thèse de doctorat, Université Sidi Mohamed Ben Abdellah.
[21]. Diakhate A. L. (2017): Cartographie des caractéristiques hydrodynamiques du système aquifère du littoral nord par l'utilisation de la théorie des variables régionalisées : cas particulier de la transmissivité. Mémoire Master 2 Génie et énergies renouvelables option Génie Civil, Ecole polytechnique de Thiès, 2017.
[22]. Ilias, B., Abdelkader, L., Mohamed, F. (2015): Estimation de la conductivité hydraulique de la nappe de tafilal et par analyse géostatistique (sud-est du Maroc). European Scientific Journal January 2015 édition vol.11, No.3 ISSN: 1857 – 7881(Print) e - ISSN 1857- 7431.
[23]. Arnaud, M., Emery X. (2000) : Estimation et interpolation spatiale: méthodes déterministes et méthodes géostatistiques. Paris : Hermès, 221 p.
[24]. ESRI. (2001-2003): (Environmental Systems Research Institute, ArcGIS 9): Using ArcGis Geostatistical Analyst. Environmental Systems Institute.
[25]. Arnaud, M., Emery X. (2000) : Estimation et interpolation spatiale: méthodes déterministes et méthodes géostatistiques. Paris : Hermès, 221 p.